http://dx.doi.org/10.5012/bkcs.2014.35.5.1312

Development of Palladium, Gold and Gold-Palladium Containing Metal-Carbon Nanoreactors: Hydrogen Adsorption

Vishal J. Mayani, Suranjana V. Mayani, and Sang Wook Kim*

*Department of Advanced Materials Chemistry, College of Science and Technology, Dongguk University−Gyeongju, Gyeongbuk 780-714, Korea. *E-mail: swkim@dongguk.ac.kr*
Received December 3, 2013, Accepted January 3, 2014

Metal-carbon nanoreactors (MCNRs) were prepared from a pristine carbon cage (CC) using a simple and efficient template method with nano silica ball (NSB), pyrolysis fuel oil (PFO) and transition metals, such as palladium and gold. Metal nanoparticles were embedded in approximately 25 and 170 nm sized, highly ordered carbon cages. The newly developed Pd, Au and Au–Pd doped carbon nanoreactors were characterized by microanalysis, N_2 adsorption–desorption isotherm, powder X-ray diffraction (XRD), thermo-gravimetric analysis (TGA), scanning electron microscopy coupled with energy dispersive spectroscopy (SEM-EDS), transmission electron microscopy and inductively coupled plasma (ICP) analysis. The ordered MCNRs have exhibited dynamic hydrogen adsorption capability compared to the carbon cage.

Key Words : Carbon cage, Hydrogen adsorption, Metal carbon nanoreactors, Metal-doped

Introduction

Designed metal-attached porous carbon materials have been newly studied extensively because of their unique porous structure, peculiar surface properties, mass transfer capability and multiple applications.[1] Transition metal supported porous carbon materials have become a promising prospective in the field of energy storage, heterogeneous catalysis and materials science owing to their size and chemical and physical properties. The efficient and economical preparation of porous carbon material is needed for the large-scale consumption of pyrolysis fuel oil (PFO) residue for new materials and devices in areas, such as adsorption, catalysis, electrochemistry, biosensors and energy related applications.[2] Porous carbon materials have some interesting physicochemical properties of their own,[3] and can be used for the template construction of metal-carbon nanoreactors (MCNRs).[2d,4] Porous carbon cage (CC) can be exploited as metal supports where catalytically active metal particles are present on the outer surface or found inside the CC. The preparation of metal decorated carbon materials using chemical methods is still based largely on expensive and tedious traditional preparation techniques, such as wet chemical impregnation,[5] self-assembly,[6] electro-deposition,[7] and physical vapor deposition.[8] The activity of metal composite materials is dependent on the nature of their interaction with porous carbon and the fundamental properties of the carbon material. Porous carbon is normally functionalized using harsh oxidative processes, such as heating in a mixture of HNO_3 and H_2SO_4 under reflux to produce defects in the carbon framework. These imperfections can serve as anchor groups for functionalization and can offer sites for co-ordination chemistry.[9] On the other hand, the introduction of a large number of flaws reduces the electrical conductivity and corrosion resistance of the resulting carbon material. Therefore, the key challenge is to develop an effectively active functionalization technique that can not only offer high density and homogeneous functional groups but produce no structural damage to the pristine carbon.[10] Among the many methods for fabricating MCNRs, the modern template method and metal doping techniques can afford a range of porous structures with a wide range of pore sizes and well-defined morphologies with metal functionality.[11] Reusable, inexpensive, and eco-friendly metal composite carbon materials have attracted considerable interest as an alternative to incompatible composite materials. Significant research is carried out to attach metal particles, such as Au, Pt, Pd, Cu, Ni, K, Mn, Pd, Pt, Ru, *etc*., to the carbon framework for potential applications in the field of catalysis and energy storage.[2c,2d,4-8,12] The sets of uniform pore sizes and adequate surface areas, as well as the addition features achieved by combining active metal particles with pristine CC, highlight the possibility of improving or promoting the activity and selectivity of MCNRs. MCNRs with hydrogen adsorption performance at room temperature and normal operating pressure (< 200 bar) are a new target for practical storage applications.[2b,3b,13]

To design MCNRs, a multi component assembly soft templating process has been modified and developed based on our previous work, which will allow large-scale production and ordered porous carbon materials.[14a] Herein, we report a simple strategy for preparing new and ordered Au/Pd doped carbon using silica spheres as the template and PFO residue as the carbon source. The hydrogen adsorption performance of the MCNRs was assessed successfully at 298 K.

Experimental

Metal-carbon nanoreactors (MCNRs) and their precursors

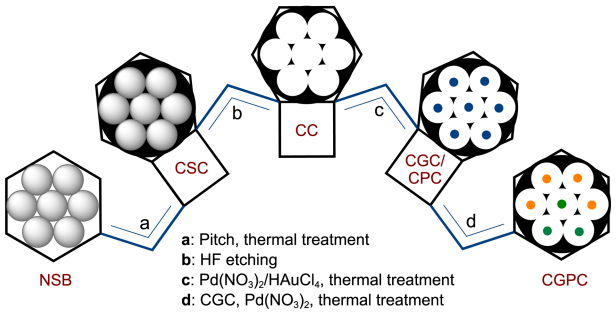

Figure 1. Schematic illustration for the synthesis of CGC, CPC and CGPC.

were synthesized as shown schematically in Figure 1. The synthesis procedure of NSB-25/170, CC-25/170 and CGC-25/170 are described in the supporting information.

Reagents, Standards and Samples. Reagents such as ethanol, toluene, ammonium hydroxide, sodium citrate dehydrate, (Dae-Jung Chemicals & Metals Co. Ltd., Korea), sodium borohydride ($NaBH_4$), tetraethylorthosilicate (TEOS), palladium nitrate dehydrate ($Pd(NO_3)_2{\cdot}2H_2O$) (Aldrich, USA), hydrofluoric acid (J. T. Baker, USA) and hydrogen tetrachloroaurate (III) hydrate ($HAuCl_4$) (Kojima Chemicals Co. Ltd, Japan) were used as received. Pyrolysis fuel oil (PFO) was purchased from the Yeocheon Naphtha Cracking Center (YNCC) Korea. All solvents were purified using known methods.[14b]

Characterization and Measurements. Hybrid metal nanocomposites of gold, palladium and gold-palladium with two sizes (~25 and ~170 nm) were characterized by powder X–ray diffraction (PXRD, Phillips X'pert MPD, Almelo, The Netherlands) over the 2θ ranges (1–10 and 10–80) at scan step 0.02°. Fourier transform infrared (FT-IR, Perkin–Elmer Spectrometer, Massachusetts, USA) spectroscopy was carried out using a KBr self–supported pellet technique. Microanalysis of the products was determined using a CHN analyzer (CE instruments, UK) and metals entering the carbon cage were determined by inductively coupled plasma–optical emission spectroscopy (ICP–OES, JY Ultima 2CHR). The BET surface area was obtained from by N_2 adsorption-desorption data measured at 77 K using a volumetric adsorption set up (Micromeritics ASAP-2010, USA). The pore diameter of the samples was determined from the desorption branch of the nitrogen adsorption isotherms using the Barret–Joyner–Halenda (BJH) model. The thermal properties of the samples were examined by thermo–gravimetric analysis (TGA, SDT600, TA instrument, USA). The microstructure was observed by scanning electron microscopy coupled with energy dispersive spectroscopy (SEM–EDS, LEO–1430, VP, UK) and transmission electron microscopy (TEM, JEM 2011, Jeol Corporation, Japan). The hydrogen adsorption isotherms were performed using gravimetric measurement with a Rubotherm MSB by following four steps: blank measurement, loading and reactivation of samples, buoyancy measurement and adsorption measurement.

Synthesis of the Carbon Palladium Composite (CPC-25/170). CC-25/170 (3 g) was placed in 100 mL of distilled water. Subsequently, 100 mL (0.5 wt %) palladium nitrate dehydrate ($Pd(NO_3)_2{\cdot}2H_2O$) solution was added and the mixture was sonicated for 1 h. The mixture was then heated for 3 h at boiling temperature. A 2% sodium borohydride ($NaBH_4$) solution (in water) was then added dropwise (50 mL). The mixture was dried in air at 110 °C and activated at 800 °C for 30 min in a tubular furnace in an argon atmosphere. After activation, the carbon was cooled to room temperature in flowing argon. To remove the excess salt, the samples were washed extensively with hot water in a Soxhlet extractor until the pH of the washing become neutral. The sample was then dried in an oven at 110 °C.

Synthesis of the Carbon Gold Palladium Composite (CGPC-25/170). A 0.5 wt % palladium nitrate dehydrate ($Pd(NO_3)_2{\cdot}2H_2O$) solution 100 mL was added to a mixture of distilled water (100 mL) and 3 g of CGC-25/170 and sonicated for 1 h. The process was followed by heating for 3 h at boiling temperature. A 2% sodium borohydride ($NaBH_4$) aqueous solution was then added dropwise (50 mL). The mixture was dried in air at 110 °C and activated at 800 °C for 30 min in a tubular furnace in an argon gas purging. Later, the resulting carbon was cooled to room temperature in flowing argon. In order to remove excess salt, the samples were treated continuously with hot water in Soxhlet extractor until the pH of the washing become neutral. The sample was then dried in oven at 110 °C.

Results and Discussion

Characterization. The palladium, gold and gold-palladium incorporated carbon nanocomposites were fully characterized by microanalysis, N_2 adsorption–desorption isotherm, SEM–EDS, TEM, ICP, TGA, PXRD and FTIR (See supporting information). The data on BET surface area, BJH pore diameter, total pore volumes found are summarized in Table 1 and also explained in supporting information.

Characterization by Powder X-ray Diffraction. Low-angle and wide-angle powder X-ray diffraction (PXRD) was used to characterize the MCNRs. Low-angle PXRD (1–10°) did not produce any characteristic peak, which indicates the

Table 1. Physico-chemical data of NSB, CC and MCNRs (~25 and ~170 nm)

Sr. No.	Compound	BET Surface Area (m^2/g)	Total Pore Volume (cm^3/g)	BJH Pore Diameter (Å)	Langmuir Surface Area (m^2/g)
1	NSB-25	30	0.086	116	38
2	CC-25	82	0.120	58	105
3	CGC-25	75	0.108	57	96
4	CPC-25	66	0.095	58	87
5	CGPC-25	63	0.092	58	81
6	NSB-170	163	0.290	71	219
7	CC-170	212	0.857	162	271
8	CGC-170	184	0.737	160	246
9	CPC-170	178	0.584	131	238
10	CGPC-170	218	0.786	144	292

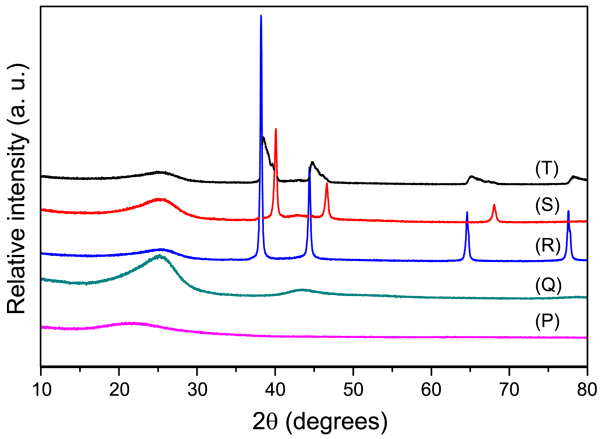

Figure 2. Wide-angle PXRD patterns of NSB-170 (P), CC-170 (Q), CGC-170 (R), CPC-170 (S) and CGPC-170 (T).

short range order or disordered phases present in the all MCNRs prepared (see supporting information). The wide-angle PXRD profile of NSB-170 showed (Figure 2(P)) a single broad peak assigned at 2θ = 21.3°, corresponding to the diffraction peak of amorphous silica.[15a] Upon switching to CC-170 (Figure 2(Q)) from NSB-170, two additional peaks, with lower intensity were observed at 2θ values of 25.2° and 43.2° corresponding to the graphite-type reflection from the (002) and (100) planes.[15a,15b] XRD of the CGC-170 material revealed four additional peaks at 2θ = 38.2°, 44.4, 64.6° and 77.6°, which were assigned to the Au planes (111), (200), (220) and (311), respectively (Figure 2(R)), denoting the formation of noble gold particles with a face centered cubic structure.[15c] Similarly, the XRD pattern of the CPC-170 composite revealed three additional peaks at 2θ = 40.1°, 46.6° and 68.1°, which corresponded to reflections of Pd planes (111), (200), (220), respectively (Figure 2(S)),[15d] signifying the face-centered cubic structure of palladium. The collective MCNRs composite CGPC-170 showed combined XRD peaks at 2θ = 38.5°, 39.6°, 44.7°, 46.1°, 65.1°, 68.0° and 78.2°, which corresponded to reflections of the Pd-Au planes (Figure 2(T)). All the MCNRs exhibited broad peaks centered at 2θ value of around 20–30° which is consistent with the typical amorphous nature of the silica/carbon foundation.

Characterization by TEM Analysis. High magnification TEM images of the NSB-25 template (Figure 3(a)) and replicated composite CC-25 (Figure 3(b)), showed that the porous structure of the silica template has been replicated. The consistent hollow cores of the hierarchically porous CC-25 were identical and strongly connected to each other.[16a]

The TEM image of CGC-25 and CPC-25 confirmed that the Au and Pd nanoparticles were dispersed homogeneously and adhered to the carbon cage cores (Figures 3(c) and 3(d)). The TEM image of CGPC-25 revealed combined Au and Pd nanoparticles on the interconnected hierarchically hollow cores (~25 nm) of the carbon structure (Figures 3(e) and 3(f)).

Nitrogen Adsorption-Desorption Study. Table 1 lists the data on the BET surface area, BJH pore diameter, total pore

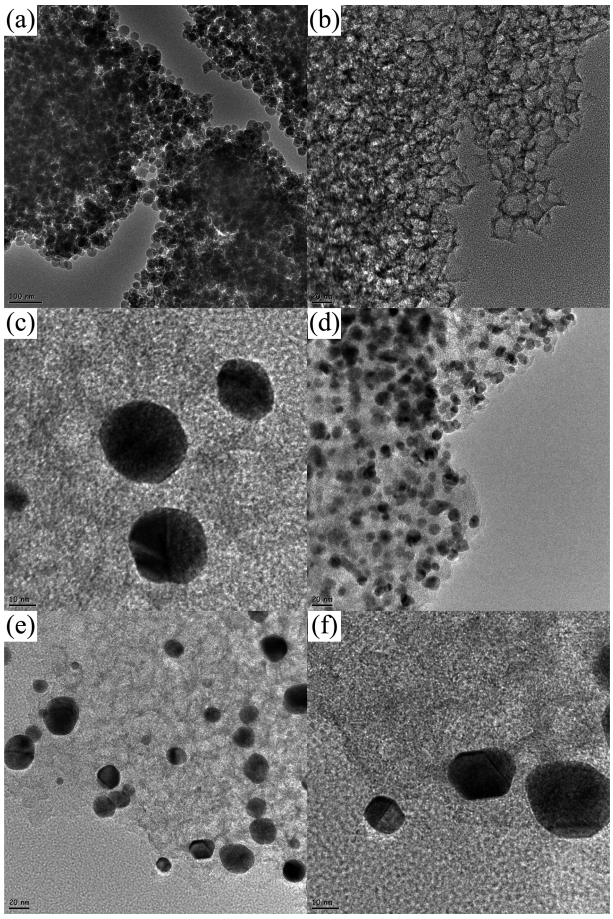

Figure 3. TEM images of NSB-25 (a), CC-25 (b), CGC-25 (c), CPC-25 (d) and CGPC-25 (e and f).

volumes and the typical isotherms of NSB, CC, CGC, CPC and CGPC (size ~25 and ~170 nm) are reported in supporting information (Figures 11-15). The NSB-25 showed fair BET surface area (30 m^2/g), total pore volume (0.086 cm^3/g) and BJH pore diameter (116 Å). A large increase in the BET surface area was observed (from 30-82 m^2/g) upon the preparation of the carbon cage (CC-25). Consequently, a decrease in the BJH pore diameter (from 116 to 58 Å) and small increase in total pore volume (from 0.086 to 0.120 cm^3/g) were observed. On the another hand, a small decrease in BET surface area (from 82 to 75 m^2/g), pore volume (from 0.120 to 0.108 cm^3/g) and pore diameter (from 58 to 57 Å) were observed upon gold incorporation in carbon cage indicates that the internal pores of the CC-25 are occupied by gold particles (CGC-25). Similarly, small decrease in BET surface area (from 82 to 66 m^2/g), pore volume (from 0.120 to 0.095 cm^3/g) and unchanged pore diameter (from 58 to 58 Å) were noticed upon palladium addition in the carbon cage indicates that the internal pores of the CC-25 are occupied by palladium particles (CPC-25). Moreover, the tiny decrease in BET surface area (from 75 to 63 m^2/g) and pore volume (from 0.108 to 0.092 cm^3/g) and the small increase in pore diameter (from 57 to 58 Å) in CGC-25 were observed which were attributed to palladium incorporation. This supports the suggestion the internal pores of CGC-25

being filled with palladium.

NSB-170 had reasonable BET surface area (163 m^2/g), total pore volume (0.290 cm^3/g) and BJH pore diameter (71 Å). A large increase in BET surface area was observed (from 163-212 m^2/g) upon the preparation of CC-170. Consequently, the BJH pore diameter (from 71 to 162 Å) and total pore volume (from 0.290 to 0.857 cm^3/g) increased. On the other hand, a small decrease in the BET surface area (from 212 to 184 m^2/g), pore volume (from 0.857 to 0.737 cm^3/g) and pore diameter (from 162 to 160 Å) were noticed upon gold incorporation in CC-170, which suggests that the internal pores of the CC-170 were occupied by gold particles (CGC-170). Similarly, a small decrease in the BET surface area (from 212 to 178 m^2/g), pore volume (from 0.857 to 0.584 cm^3/g) and pore diameter (from 162 to 131 Å) were observed upon palladium addition in the carbon cage indicating that the internal pores of the CC-170 were occupied by palladium particles (CPC-170). Moreover, small increase in the BET surface area (from 184 to 218 m^2/g), pore volume (from 0.737 to 0.786 cm^3/g) and small decrease in pore diameter (from 160 to 144 Å) were observed upon palladium incorporation in CGC-170, also suggesting that the internal pores of the CGC-170 were occupied by palladium particles (CGPC-170). This suggests that the structure of MCNRs are maintained after modification.

Hydrogen Adsorption Study. The hydrogen adsorption isotherms were obtained by gravimetric measurements using a Rubotherm MSB in the following four steps: blank measurement, loading and reactivation of samples, buoyancy measurement and adsorption measurement. The adsorption measurements at 25 °C were performed at pressure up to 80 bar. The samples were activated in situ by controlled heating up to 400 °C (heating range 1 °C/min) under high vacuum and the temperature and vacuum were maintained for 12 h before the adsorption measurements. The amount of activated adsorbent was determined from the weight of the absorbent before and after activation and prior to start of the adsorption measurements. After activation, the samples were allowed to cool to the desired temperature and the temperature was maintained during the entire analysis using an external water circulator. Hydrogen with specific pressure steps was introduced into the sample chamber. The increased weight of the sample due to hydrogen adsorption was measured accurately using MSB connected to the sample holder. Typically, 0.2–0.7 g of the samples were used in the experiment. The adsorption isotherms of CC-25, CC-170, CGC-25, and CGC-170 were conducted to determine the enhancement of modified carbon. The hydrogen adsorption capacity of all compounds is expressed in terms of wt % (weight of the hydrogen molecules/weight of the material × 100).

The adsorption of hydrogen in pristine CC-25, CC-170 and CGC-170 were examined using a static gravimetric adsorption system. Figures 4 and 5 show the experimental hydrogen uptake of CC-25/170 and CGC-25/170 capacities at 25 °C and pressure up to 80 bar. The adsorption of hydrogen occurred in the potential region that restrained the hydrogen adsorption domain. The hydrogen adsorption of

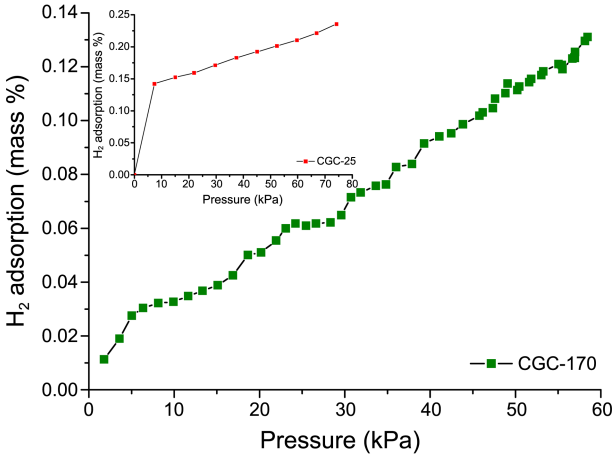

Figure 4. Hydrogen adsorption isotherms of CGC-25 and CGC-170.

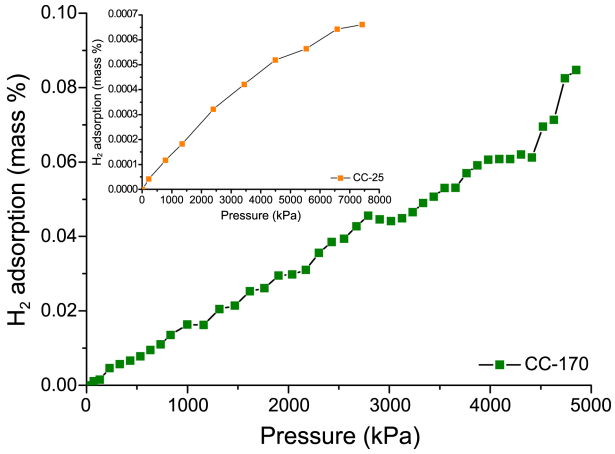

Figure 5. Hydrogen adsorption isotherms of CC-25 and CC-170.

CGC-25 and CGC-170 showed a maximum hydrogen adsorption capacity of 0.13 wt % (58.5 kPa) and 0.24 wt % (74.2 kPa), respectively. The adsorption capacity of CGC-25/170 increased with increasing pressure at room temperature. On the other hand, hydrogen adsorption was absent for pristine CC-25 and CC-170 at pressures up to 8000 kPa and 5000 kPa, respectively because of the weak interaction between H_2 and pristine carbon (CC), leading to hydrogen molecular adsorption, which can be useful for storage only at temperatures around that of liquid nitrogen. The adsorption performance of pure carbon at room temperature and normal pressure still remained far below the desirable targets for practical storage applications compared to MCNRs. In general, the experimental results show that the hydrogen adsorption ability of the MCNRs (CGC-25/170) was improved significantly compared to that of the non-metal CC-25 and CC-170 base, in terms of the percentage mass uptake per unit pressure (Figure 5). The gold-deposited MCNRs can lead to a higher hydrogen storage compared to the pristine carbon cage (CC-25/170) as a result of the weak chemisorptions process initiated by the so-called "spillover" effect.[16b,16c]

Conclusions

Pd, Au and Au-Pd doped carbon composites (MCNRs), with combination of two different sized carbon cages, were synthesized and characterized. The designed MCNRs and pristine CC have potential applications in adsorption due to their collective chemical and physical properties. CGC-25 and CGC-170 showed a remarkable hydrogen adsorption capacity at ambient temperature and normal operating pressures (< 200 bar). These MCNRs can be used as a heterogeneous catalyst and adsorbent for energy storage and reverse 'greenhouse' effect. Experiments aimed at developing new techniques for ideal MCNRs that will enhance the adsorption and storage capacities are currently underway.

Acknowledgments. This work was supported by the National Research Foundation of Korea (NRF) grant funded by the Korea Government (MSIP) (NRF- 2013M2A2A7059045) and Dongguk University–Gyeongju Research Fund.

Supplementary Data. Supplementary data associated with this article can be found in the online version.

References

1. Zhao, X. C.; Wang, A. Q.; Yan, J. W.; Sun, G. Q.; Sun, L. X.; Zhang, T. *Chem. Mater.* **2010**, *22*, 5463.
2. (a) Lee, K. T.; Lytle, J. C.; Ergang, N. S.; Oh, S. M.; Stein, A. *Adv. Funct. Mater.* **2005**, *15*, 547. (b) Cao, D.; Feng, P.; Wu, J. *Nano Lett*. **2004**, *4*, 1489. (c) Hrapovic, S.; Liu, Y.; Male, K. B.; Luong, J. H. T. *Anal. Chem.* **2004**, *76*, 1083. (d) Mayani, S. V.; Mayani, V. J.; Lee, J. Y.; Ko, S. H.; Lee, S. K.; Kim, S. W. *Adsorption* **2013**, *19*, 251.
3. (a) Baughman, R. H.; Zakhidov, A. A.; Heer, W. A. *Science* **2002**, *297*, 787. (b) Rao, C. N. R.; Satishkumar, B. C.; Govindaaj, A.; Nath, M. *Chem. Phys. Chem.* **2001**, *2*, 78.
4. (a) Planeiz, J. M.; Coustel, N.; Coq, B.; Brotons, V.; Kumbhar, P. S.; Dutartre, R.; Geneste, P.; Bernier, P.; Ajayan, P. M.; *J. Am. Chem. Soc.* **1994**, *116*, 7935. (b) Che, G. L.; Lakshmi, B. B.; Martin, C. R.; Fisher, E. R. *Langmuir* **1999**, *15*, 750. (c) Rajesh, B.; Thampi, K. R.; Bonard, J. M.; Viswanathan, B. *J. Mater. Chem.* **2000**, *10*, 1757. (d) Lordi, V.; Yao, N.; Wei, J. *Chem. Mater.* **2001**, *13*, 733.
5. Zhang, R. Y.; Wang, X. M. *Chem. Mater.* **2007**, *19*, 976.
6. Rahman, G. N. A.; Guldi, D. M.; Zambon, E.; Pasquato, L.; Tzitzios, V.; Gournis, D.; Petridis, D. *Small* **2005**, *1*, 527.
7. Quinn, B. M.; Dekker, C.; Lemay, S. G. *J. Am. Chem. Soc.* **2005**, *127*, 6146.
8. Zhang, Y.; Dai, H. J. *Appl. Phys. Lett.* **2000**, *77*, 3015.
9. Xing, Y.; Li, L.; Chusuei, C. C.; Hull, R. V. *Langmuir* **2005**, *21*, 4185.
10. Zhao, Y.; Yang, X.; Zhan, L.; Ou, S.; Tian, J. *J. Mater. Chem.* **2011**, *21*, 4257.
11. (a) Xia, K.; Gao, Q.; Jiang, J.; Wang, H. *Mater. Lett.* **2013**, *100*, 127. (b) Chen, W. X.; Lee, J. Y.; Liu, Z. *Mater. Lett.* **2004**, *58*, 3166. (c) Zhao, X. S.; Su, F.; Yan, Q.; Guo, W.; Bao, X. Y.; Lv, L.; Zhou, Z. *J. Mater. Chem.* **2006**, *16*, 637.
12. Ravat, V.; Nongwe, I.; Meijboom, R.; Bepete, G.; Coville, N. J. *J. Catal.* **2013**, *305*, 36.
13. Wang, L.; Yang, R. T. *Catal. Rev.* **2010**, *52*, 411.
14. (a) Mayani, S. V.; Mayani, V. J.; Park, S. K.; Kim, S. W. *Mater. Lett.* **2012**, *82*, 120. (b) Perrin, D. D.; Armarego, W. L. F.; Perrin, D. R. *Purification of Laboratory Chemicals*; Pergamon: New York, 1981.
15. (a) Guo, X.; Liu, X.; Xu, B.; Dou, T. *Colloids Surf. A* **2009**, *345*, 141. (b) Kao, L. H.; Hsu, T. C.; *Mater. Lett.* **2008**, *62*, 695. (c) Vermisoglou, E. C.; Romanos, G. E.; Tzitzios, V.; Karanikolos, G. N.; Akylas, V.; Delimitis, A.; Pilatos, G.; Kanellopoulos, N. K.; *Microporous Mesoporous Mater.* **2009**, *120*, 122. (d) Giasafaki, D.; Charalambopoulou, G.; Bourlinos, A.; Stubos, A.; Gournis, D.; Steriotis, T. *Adsorption* **2013**, *19*, 803.
16. (a) Li, Q.; Jiang, R.; Dou, Y.; Wu, Z.; Huang, T.; Feng, D.; Yang, J.; Yu, A.; Zhao, D. *Carbon* **2011**, *49*, 1248. (b) Contescu, C. I.; Benthem, K. V.; Li, S.; Bonifacio, C. S.; Pennycook, S. J.; Jena, P.; Gallego, N. C. *Carbon* **2011**, 49, 4050. (c). Jimenez, V.; Ramırez-Lucas, A.; Sanchez, P.; Valverde, J. L.; Romero, A. *Int. J. Hydrogen Energy* **2012**, *37*, 4144.